VIP Plasma Chemistry

DOI: 10.1002/anie.200802891

Nanoscale Corona Discharge in Liquids, Enabling Nanosecond Optical Emission Spectroscopy**

David Staack, Alexander Fridman, Alexander Gutsol, Yury Gogotsi, and Gary Friedman**

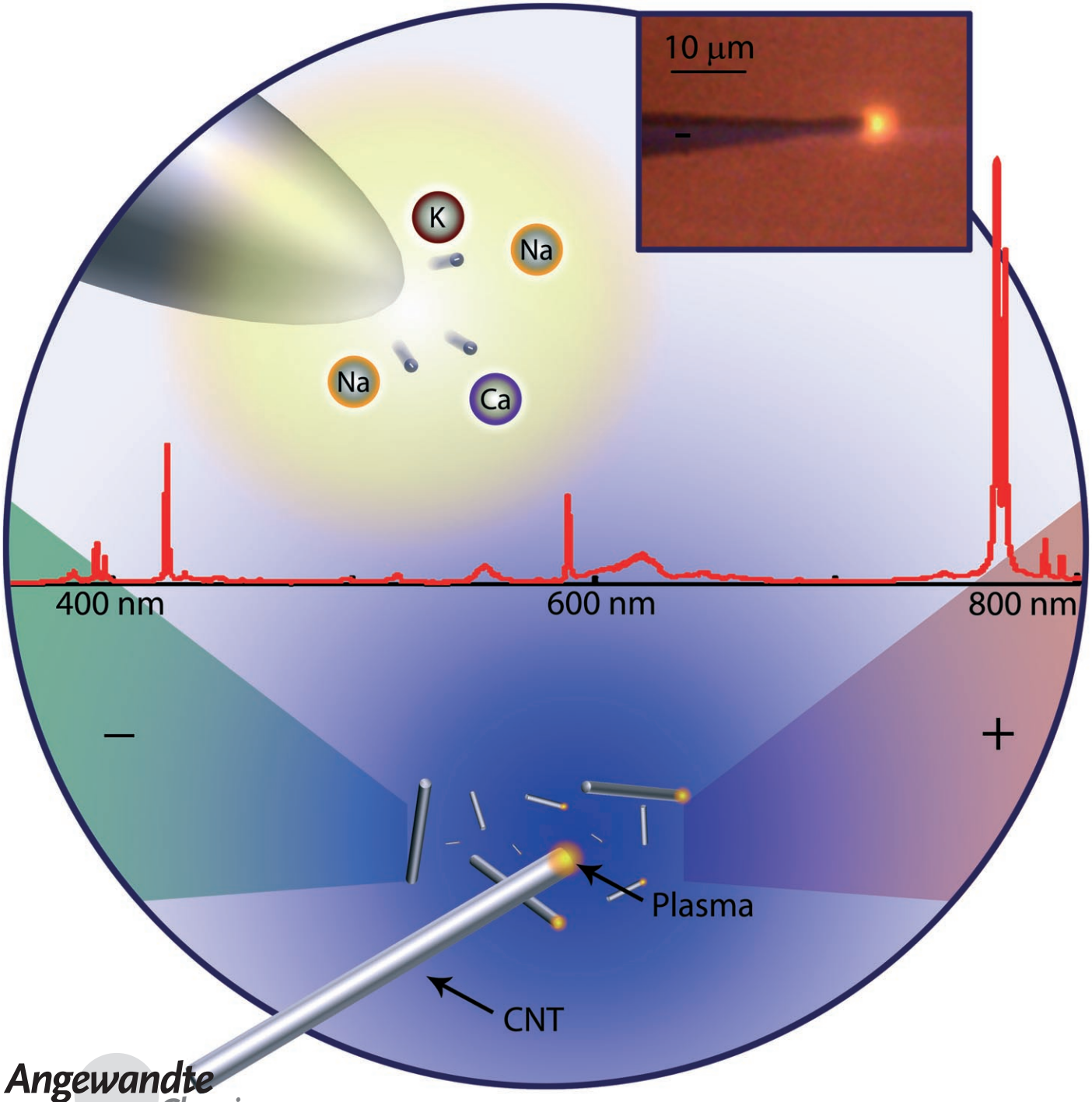

Electrical discharges in liquids have been studied for purposes[1] ranging from dielectric insulation to material synthesis, destroying microorganisms, and tissue ablation. However, the plasma in these discharges has always been hot, or thermal.[2] Cold (nonthermal) plasmas in the gas phase require a macroscopic volume to provide enough mean free paths for electron multiplication. Denser liquid media could create nanoscale nonthermal plasmas, but such a plasma in water has never been reported.[2] Reported herein for the first time is a nonthermal corona discharge in liquid around electrodes with ultrasharp tips and around elongated nanoparticles (nanowires). Plasmas created with 50 nm probe tips or carbon nanotubes (CNTs) dispersed in solutions allow simultaneous chemical analysis of multiple dissolved elements within nanoseconds. The proposed optical emission spectroscopy (OES) method can be applied for ultrafast time-resolved multielemental analysis of liquid in microfluidic reactors, living biological systems, or environmental sensors and for diagnostics of femtoliter volumes with one micrometer or better spatial resolution. Using this method, we have detected part-per-million concentrations of sodium, calcium, and other elements in aqueous solutions.

Transient sparks and streamer corona discharges occur in liquid medium,[1,3] typically initiated by the rapid application of high electric field between macroscopic electrodes in the liquid. The exact mechanisms causing initiation of these plasmas are still unclear. In most cases, bubbles grow and rapidly propagate through the liquid as branched streamers. When the streamers reach the counter electrode, sparks with typical power dissipation of kilojoules per pulse form. Lower powers (joules per pulse) result in an incomplete discharge, the streamer corona. Thermal plasma formation and phase change in such discharges result in generation of shocks, and OES shows many overlapping lines and significant stark broadening of the hydrogen Balmer lines owing to the high electron density.

By contrast, it is demonstrated herein that a nonthermal plasma can be created around ultrasharp tips and nanotubes (referred to herein as nanoscale corona discharge probes or NCDPs) with much lower powers (millijoules per pulse) and without streamers. Time-resolved OES of NCDPs demonstrates narrow spectral lines that prove very useful for simple yet sensitive multielemental analysis, thus opening new possibilities in chemical detection, environmental monitoring, medicine, and many other applications.

Electrochemical probes can measure the concentration of specific ions in electrolyte solution and can be scaled down to micrometers,[4] but they are relatively slow and inefficient for measuring multiple ions. Optical techniques, such as UV/Vis absorption spectroscopy, provide only indirect information about the chemical composition (no elemental analysis) and need calibration. Sensitive fluorescent techniques used in cell biology for measuring calcium and other ions are highly application-specific and can themselves affect ion concentrations.[5] OES is probably the most common method for quantitative analysis[6,7] of liquid solutions. Such state-of-the-art techniques as laser-induced breakdown spectroscopy (LIBS)[8–10] have been shown to analyze nanoliter volumes with levels of detection (LOD) in water of part per million (ppm). However, LIBS is complicated by the need for multiple laser pulses and the need for focusing and switching a powerful laser, requiring relatively large instruments. Glow discharge OES[11] requires aspiration of the solution into the plasma region and uses larger volumes (mL). By contrast, OES obtained from NCDPs requires only a low-power generator, which can fit into the palm of a hand. Moreover, NCDP spectroscopy can be performed remotely without electrical connections when nanoparticles are used as probes. OES can be easily collected from tiny volumes as well as from liters of flowing or static solution.

In a typical experiment (Figure 1), a tungsten wire with a tip sharpened to below 50 nm radius was used to generate the corona discharge. Alternatively, carbon fibers with a diameter of approximately 4 μm, quartz pipettes with 0.5–1 μm tips covered by a gold film, and template-grown noncatalytic chemical vapor deposition (CVD) CNTs of 200 nm diameter[12] were employed. Negative corona discharges at the tips

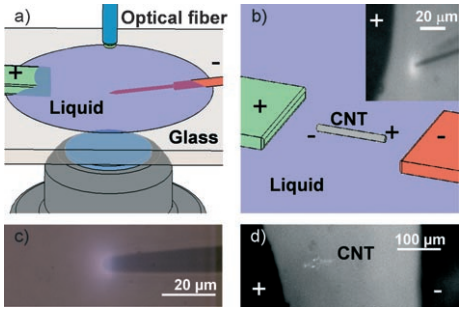

Figure 1. Direct (a) and remote (b) setups for micro- and nanoscale corona discharge OES. a) An electrically wired probe with tip sharpened to 100 nm diameter immersed in a grounded fluid. Discharge is observed by microscope and spectra are collected through an optical fiber. b) Disconnected high aspect ratio, highly polarizable object, such as a CNT, in fluid. Bias on remote electrodes induces fields and creates corona discharge. Inset shows an induced corona around a 4 μm carbon microfiber in water. c, d) Optical micrographs of typical coronas around a wire tip and a bundle of multiwalled carbon nanotubes.

[*] Prof. Y. Gogotsi
Department of Materials Science and Engineering
Drexel University, Philadelphia, PA 19104 (USA)
Fax: (+1) 215-895-1293
E-mail: gogotsi@drexel.edu
Homepage: http://nano.materials.drexel.edu
Prof. G. Friedman
Department of Electrical and Computer Engineering
Drexel University, Philadelphia, PA 19104 (USA)
E-mail: gary@coe.drexel.edu
D. Staack, Prof. A. Fridman, Prof. A. Gutsol
Department of Mechanical Engineering and Mechanics, Drexel University

[**] This work was supported by a W.M. Keck Foundation grant to establish the Keck Institute for Attofluidic Nanotube-Based Probes at Drexel University. The authors would like to thank J. Giammarco for producing carbon nanotubes, T. Farouk, B. Farouk (all Drexel University), and J.E. Fischer (University of Pennsylvania) for helpful discussions.

Supporting information for this article is available on the WWW under http://dx.doi.org/10.1002/anie.200802891.

have been demonstrated in all cases. The pulsed voltage source (see the Supporting Information for details) provides 2–30 kV pulses 10–500 ns in duration at approximately 30 Hz repetition rate. Negative corona was achieved for a 50 nm radius tip with as little as 3 kV. This field is comparable to the field of $1.28 \times 10^{10}\ \mathrm{V\,m^{-1}}$ needed for electron emission from tungsten. These field-emission-initiated negative coronas require nanoscale electrodes and are not observed when macroscale electrodes or positive polarities are used.

Direct and remote methods of generating NCDPs were considered. In one, the probe is directly connected to the voltage source (Figure 1a). In other cases, isolated CNTs, CNT bundles, or short carbon fibers were placed in liquid, and the voltage source was used to create electric field pulses (Figure 1b). The CNTs polarize, and a corona is observed only on the negative tip. This new regime of remote generation eliminates the need to wire nanoscale objects and opens up numerous potential applications. Single nanotubes placed in liquids produce faint sub-micrometer bright spots and move when voltage is applied (see the Supporting Information), but the bright spots are only recorded with intensified CCD cameras. A clearer image with multiple spots coming from a CNT bundle illustrates the remote discharge (Figure 1d).

Initial observations showed that discharges in tap water and salt water give coronas of different colors (Figure 2a,b), suggesting that they can be used for spectroscopic measurements. Indeed, OES clearly shows the presence of different elements (Figure 2c–e), allowing us to uniquely distinguish solutions of different salts. Visible differences in the discharges were also apparent for different pulse durations. For pulse durations of 20 ns, a discharge with a diameter of less than 3 μm is visible (Figure 2f). At a pulse duration threshold of about 100 ns, the discharge increases in size to about 10 μm in diameter (Figure 2g), and bubbles are seen to emanate from the probe tip. For stepped voltages (rather than pulsed) the discharge is again larger (Figure 2b), and significant bubble formation owing to electrolysis along the wire length is visible.

The discharge variations with pulse duration were also visible in the observed spectra. For pulse durations less than 100 ns (Figure 2e), signals corresponding to elements such as H and O resulting from decomposition of the water practically disappear. This phenomenon was further investigated using time-resolved study of the light emission (Figure 3).

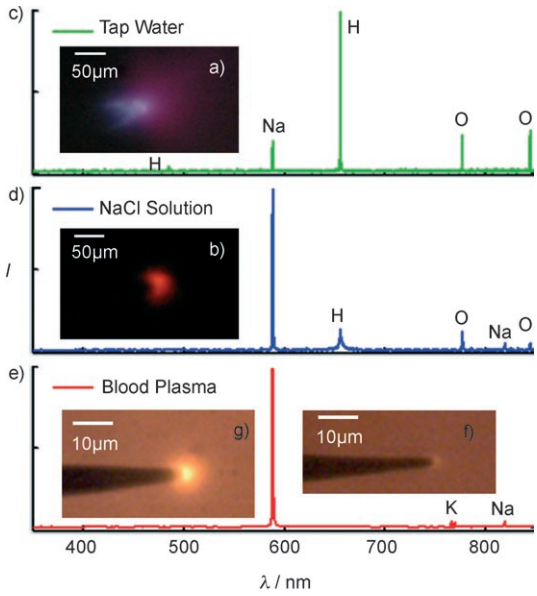

Figure 2. OES and corona discharges produced using 5 kV stepped and pulsed voltage excitation in liquids. a,b) Demonstration of color changes as a function of the composition of the solution. c,d) OES from tap water (c) and 0.5 M NaCl (d). e) OES for 5 kV, 20 ns duration pulses in blood plasma; this spectrum does not show oxygen and hydrogen peaks and indicates that for longer discharges, light emission is due to recombined ions and decomposition of the liquid, whereas in short discharges, light emission is due solely to recombined ions. Optical micrographs indicate that the short-duration pulsed coronas (f) are less than 3 μm in diameter and are significantly smaller than discharges from microsecond-duration pulses (g), for which a larger discharge and bubble formation is seen.

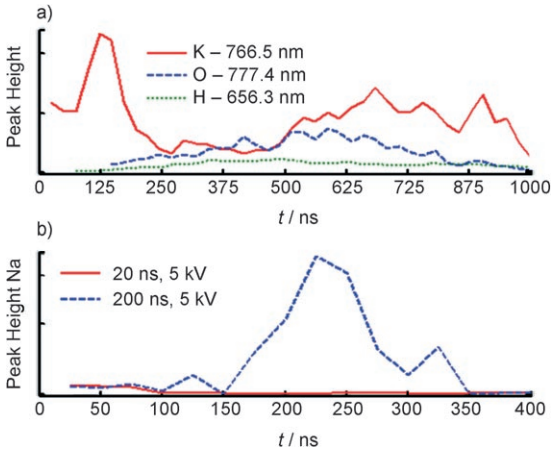

Figure 3. Time-resolved OES measurements show that the analysis is extremely fast and demonstrates regimes of the discharge. a) The intensity of K peak at 766.5 nm, O peak at 777.4 nm, and H peak at 656.3 nm compared as a function of time; the O and H peaks only arise after bubble growth (ca. 100 ns). b) Intensity of the Na line at 589 nm monitored as a function of time for short- and long-duration pulses. Comparison of 20 and 200 ns pulses shows that initially both discharges are the same, but an increase in light emission corresponding to growth of the bubble is seen at approximately 100 ns. Short-duration voltage pulses arrest the discharge in the initial phase. Camera takes 25 ns exposures and is triggered by the spark gap.

Several regimes of the discharge are apparent, the first two of which have not been observed before. Depending on the duration of the excitation pulse, the negative corona is observed to evolve through one or four stages: 1) weak pre-bubble, 2) initial bubble, 3) high-electron-density bubble, 4) relaxation. Spectral signatures only corresponding to recombined ions are visible in the first stage (less than 100 ns). For example, the peak assignments reveal that emissions occur from the electron recombined cations from the solution [Eq. (1), * denotes electronically excited states].

$$\begin{aligned} \mathrm{Na^{+}} + e^{-} &\rightarrow \mathrm{Na^{*}} \Rightarrow \mathrm{Na^{*}} \rightarrow \mathrm{Na} + hc/\lambda, \\ \mathrm{Ca^{++}} + e^{-} &\rightarrow \mathrm{Ca^{+}}{}^{*} \Rightarrow \mathrm{Ca^{+}}{}^{*} \rightarrow \mathrm{Ca^{+}} + hc/\lambda, \end{aligned} \qquad (1)$$

The mechanism may be direct or multistep, but the magnitude of the peaks corresponding to each element is linearly proportional to the molar concentration of the corresponding salt, as shown in Figure 4a.

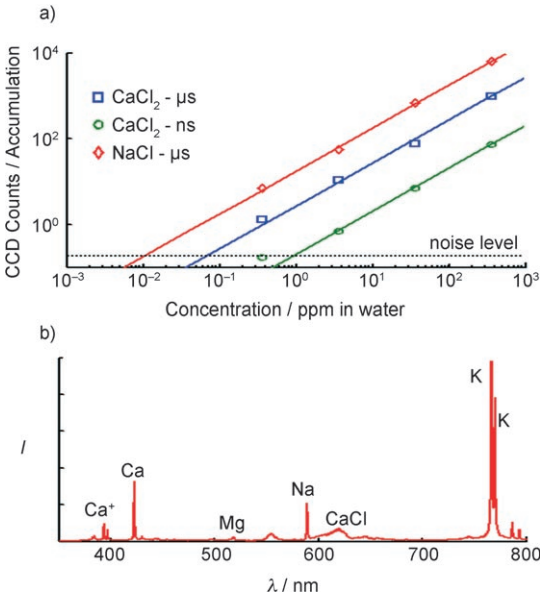

Figure 4. Analytical capabilities of short and long pulses. a) Calcium concentration can be measured to 1 ppm concentrations in volumes smaller than 10 fL using nanosecond-duration pulses. Longer (µs) pulses can detect lower concentrations from volumes smaller than 20 pL. Intensity varies linearly with concentration, and a higher sensitivity is observed for Na. b) Operation in a nonthermal regime limits the number and broadening of lines and allows multiple elements to be detected simultaneously. Using short pulses of less than 50 ns, only recombined ions are detectable. Longer pulses show both recombined ions and decomposition of the liquid.

In the second stage (100–200 ns), recombined ions as well as initial dissociation products of water (O, H, and OH) are identifiable as the bubble grows. In the third phase (200–1 µs), depending on the pulse intensity, a thermal plasma forms, the electron density and degree of water dissociation increase, and hydrogen line broadening hides the presence of other elements and spectral lines. In the fourth stage the electron density decreases and lineshapes are narrower, allowing elements to be more easily identified. The third and fourth phases are expectedly similar to the spectral evolution observed in LIBS and sonoluminescence. In such systems either the laser irradiation or sound generates a hot plasma bubble, and spectral components are identified during the relaxation phase of the bubble. In identifying lead content in solution, our detection limit is slightly better than 10 ppm in water (similar to LIBS) and is limited by overlap from OH and H lines. For the NCDP, the light emission can be arrested in just the first or second stages (Figure 3b) by shortening the pulse duration. Using only discharges in the first stages, detection limits of calcium are in the parts per million ranges in water and are limited by photon detection (Figure 4a). Longer duration discharges have detection limits in the parts per billion ranges, but are larger in size.

Considering existing theories of discharge initiation in liquids[13–15] and our current experiments, there are several factors that contribute to the reasons why the NCDP is different from the streamer coronas previously observed in liquid and specifically why the two initial stages of the negative corona are observed. This study is the first which simultaneously combines 1) short rise-time voltages, 2) nanosecond-duration pulses, 3) high temporal resolution emission spectra, and most importantly 4) nanoscale tips. The nanoscale tip allows for a slower temporal evolution of the discharge in several ways. First, there are no pre-existing microbubbles on the surface that facilitate breakdown. Second, although the power density remains constant as the electrode size is reduced to the nanoscale, relative losses increase with increasing surface-to-volume ratio $S/V \approx 1/r$, analogous to the size stabilization we have observed for microscale plasma discharges in air.[16] Lastly, with nanoscale electrodes, field emission processes are more controllable, and there is no need to rely on unknown asperities or pre-existing bubbles as in macroscale discharge devices. As such, the discharge can be operated with only very small over voltages (voltages in excess of the field emission threshold).

The results reported herein suggest numerous immediate applications for nanoscale OES probes in microanalysis, analysis of flowing fluids in chemical reactors (including factories on a chip and microfluidics chips), in cell biology for measuring calcium concentrations and understanding calcium signaling, and in environmental monitoring. As shown in Figure 4b, multiple elements can be detected simultaneously. In forensic research, detection of poisons, such as arsenic or polonium, in body fluids or extremely small amounts of food residue may be possible. The technique is more sensitive than the X-ray spectroscopy (energy-dispersive or wavelength dispersive) used in SEM for analysis of microscopic amounts of material with about the same analyzed material volume (one cubic micrometer), but it uses simpler methods. The use of smaller nanotubes[17] or other pointed carbon tips[18,19] may further decrease the analyzed volume.

In addition to diagnostics of liquids, NCDPs can be used for delicate plasma chemical processes (for example, localized functionalization, plasma-enhanced deposition of coatings, and direct nano- or micropatterning from liquids) or nanoscale welding (e.g., welding nanotubes or nanowires to a contact pad or welding two nanowires together). One-dimensional cellular probes based on carbon nanotubes and nanowires have been recently reported by several groups,[20–23] but these probes lack the capability to perform elemental analysis. In combination with the OES reported herein, these probes could become simple yet powerful analytical and diagnostic tools. Nanoscale cell surgery would be another attractive application for higher-intensity discharges at the tip of a nanotube probe.[21] Since nanotubes have been shown to penetrate cell membranes and be delivered to tumors by antibodies attached to CNT surfaces, use of remote discharge for destroying tumors can be suggested. Of course, these hypothetical applications need experimental verification.

Experimental Section

Discharge generation: A pulsed power supply was constructed using spark gaps in a configuration similar to those used in other pulse generator systems. A direct current (DC) power supply (Bertran Model 205A-50R) capable of 50 kV output and reversible polarity was connected to a resistor–capacitor (RC) charging circuit. The DC circuit charges the capacitor until the voltage is sufficient to cause breakdown across the primary spark gap. The length of the spark gap determines the voltage applied to the load. A current transformer (Pearsons model 2877) and voltage probe divider (North Star PVM-4) were used to estimate the current and voltage to the electrode. The resistance, capacitance, and power supply voltage determine the repetition rate of the discharge, which was typically between 1 and 50 Hz. A second adjustable spark gap acts to remove the voltage from the load. Variation of the length of the second spark gap adjusts the duration of the pulse. The operation of the pulsing circuit is largely independent of the load, as only a small fraction of the power goes to the load. In stepped mode all of the power must dissipate through the liquid, and the waveforms are highly dependent on the conductivity of the solution and immersed electrode geometry.

Probes: Several varieties of micro- and nanoscale electrodes were used as probes, such as commercially available electrolytically etched tungsten probes with less than 100 nm tip radii (T-4-10, GGB Industries, Inc.), carbon fibers with approximately 4 μm diameter manufactured by Energy Science Laboratories, Inc., and template-grown noncatalytic CVD carbon nanotubes of approximately 200 nm diameter. These nanotubes were used as remote electrodes both dispersed in liquid and electrostatically affixed to a polyacrylonitrile (PAN) coating.

Spectra acquisition: All spectra were acquired using a TriVista scanning monochromator system from Princeton Instruments. Light from the discharge was collected by a single optical fiber 3 m in length and 250 μm in diameter aligned with the discharge and mounted on the entrance slit of the spectrometer. Optical emission spectra of the discharge were taken in the range 200–900 nm, averaging emission from the entire discharge. An intensified CCD camera (Princeton Instruments Gen III PI-MAX 2) was mounted on the exit of the spectrometer and trigger by the measured probe voltage to digitally record the spectra. A photon-counting photomultiplier tube (R928, Hamamatsu) was mounted on the secondary spectrometer output to verify results from the ICCD camera and to calibrate its intensity.

Received: June 17, 2008
Published online: August 28, 2008

Keywords: emission spectroscopy · optical analysis · plasma chemistry · trace analysis

[1] B. Locke, M. Sato, P. Sunka, M. Hoffmann, J. Chang, *Ind. Eng. Chem. Res.* **2006**, *45*, 882.
[2] A. Fridman, *Plasma Chemistry*, Cambridge Universtiy Press, Cambridge, **2008**.
[3] W. An, K. Baumung, H. Bluhm, *J. Appl. Phys.* **2007**, *101*, 053302.
[4] K. Yum, H. N. Cho, J. Hu, M.-F. Yu, *ACS Nano* **2007**, *1*, 440.
[5] A. Minta, J. P. Kao, R. Y. Tsien, *J. Biol. Chem.* **1989**, *264*, 8171.
[6] T. Nelis, R. Payling, *Glow Discharge Optical Emission Spectroscopy: A Practical Guide*, Royal Society of Chemistry, London, **2003**.
[7] R. K. Marcus, J. A. C. Broekaert, *Glow Discharge Plasmas in Analytical Spectroscopy*, Wiley, New York, **2003**.
[8] R. L. V. Wal, T. M. Tichich, J. R. West, P. A. Householder, *Appl. Spectrosc.* **1999**, *53*, 1226.
[9] A. Assion, M. Wollenhaupt, L. Haag, F. Mayorov, C. Sarpe-Tudoran, M. Winter, U. Kutschera, T. Baumert, *Appl. Phys. B* **2003**, *77*, 391.
[10] D. A. Rusak, B. C. Castle, B. W. Smith, J. D. Winefordner, *Crit. Rev. Anal. Chem.* **1997**, *27*, 257.
[11] M. R. Webb, F. J. Andrade, G. M. Hieftje, *Anal. Chem.* **2007**, *79*, 7807.
[12] D. Mattia, M. P. Rossi, B. M. Kim, G. Korneva, H. H. Bau, Y. Gogotsi, *J. Phys. Chem. B* **2006**, *110*, 9850.
[13] T. J. Lewis, *IEEE Trans. Dielectr. Electr. Insul.* **2003**, *10*, 948.
[14] J. Quan, R. P. Joshi, K. H. Schoenbach, J. R. Woodworth, G. S. Sarkisov, *IEEE Trans. Plasma Sci.* **2006**, *34*, 1680.
[15] A. I. Gerasimov, *Instrum. Exp. Tech.* **2005**, *48*, 141.
[16] D. A. Staack, B. Farouk, A. F. Gutsol, A. Fridman, *Plasma Sources Sci. Technol.* **2008**, *17*, 025013.
[17] Y. Gogotsi, *Nanomaterials Handbook*, CRC, Boca Raton, FL, **2006**.
[18] Y. Gogotsi, S. Dimovski, J. A. Libera, *Carbon* **2002**, *40*, 2263.
[19] Y. Gogotsi, J. A. Libera, N. Kalashnikov, M. Yoshimura, *Science* **2000**, *290*, 317.
[20] N. A. Kouklin, W. E. Kim, A. D. Lazareck, J. M. Xu, *Appl. Phys. Lett.* **2005**, *87*, 173901.
[21] J. R. Freedman, G. Friedman, A. K. Fontecchio, D. Mattia, Y. Gogotsi, G. Korneva, *Appl. Phys. Lett.* **2007**, *90*, 103108.
[22] I. U. Vakarelski, S. C. Brown, K. Higashitani, B. M. Moudgil, *Langmuir* **2007**, *23*, 10893.
[23] X. Chen, A. Kis, A. Zettl, C. R. Bertozzi, *Proc. Natl. Acad. Sci. USA* **2007**, *104*, 8218.

